

Supporting Information

Design of ternary solid lubricants SiO₂/Ti₃C₂/PTFE for wear-resistant, self-lubricating polyimide composites

Guojing Chen, Shuai Jiang, Yufei Huang, Xinrui Wang, Chunpeng Chai*

School of Materials Science and Engineering, Beijing Institute of Technology, Beijing, 100081, China.

*Corresponding authors, E-mail: chaicp@bit.edu.cn

Table of Contents:

Materials

Preparation of Ti₃C₂

Preparation of SiO₂-Ti₃C₂ (ST)

Preparation of PAA

Characterization

Tribological tests

The mass ratio of Ti₃C₂T_x-SiO₂/PTFE and samples name Table S1

Tribological properties of PI composites with different SiO₂-Ti₃C₂ and PTFE mass ratios Fig. S1

Roughness value of the STP/PI samples Table S2

AFM image of PI Fig. S2

Friction performance of TP/PI and STP/PI samples Fig. S3

Average wear rate of T/PI with different Ti₃C₂ content Fig. S4

Average coefficient of friction of ST/PI with different Ti₃C₂@SiO₂ contents Fig.S5

XPS spectrum of transfer film on steel ball Fig. S6

XPS narrow spectrum of C 1s from ST/PI transfer film Fig. S7

XPS narrow spectrum (Ti 2p) of transfer film on steel ball Fig.S8

Comparison of the tribological properties of this paper with other literatures Table S3

Materials

MAX phase (Ti_3AlC_2) was purchased from Jilin 11 Technology Co, the particle size is 5 μm . HF (AR) and Homophthalic dianhydride (PMDA, AR) were purchased from Shanghai Sarn Chemical Technology Co. 4,4'-Diaminodiphenyl ether (ODA, AR), Tetraethyl orthosilicate (TEOS, AR) and Ammonia ($\text{NH}_3\cdot\text{H}_2\text{O}$, 25%~27%,) were provided by Anhui Zesheng Technology Co. Polytetrafluoroethylene (PTFE, 12 μm), Anhydrous ethanol (EtOH, AR) and N, N-Dimethylacetamide (DMAc, AR) were purchased from Tianjin Guang Fu Technology Development Co.

Preparation of Ti_3C_2

Ti_3AlC_2 (1 g) was added to HF (20 mL, 40 wt%) in batches, the stirring speed and temperature were set to 500 rpm and 35°C respectively. After 24 h of reaction, the mixed solution was washed with deionized water and centrifuged at 3500 rpm for 5 min. The above washing operation was repeated until the pH of the supernatant liquid surface was neutral. Finally, the precipitate was freeze-dried at -69°C for 8 h to obtain $\text{Ti}_3\text{C}_2\text{T}_x$.

Preparation of SiO_2 - Ti_3C_2 (ST)

$\text{Ti}_3\text{C}_2\text{T}_x$ powder (0.20 g) was ultrasonically dispersed in a mixture of anhydrous ethanol (130 mL) and deionized water (25 mL). The above mixture was magnetically stirred in a flask and $\text{NH}_3\cdot\text{H}_2\text{O}$ (6 mL) was added dropwise until the pH of the solution up to 10. TEOS (2 g) was dissolved in anhydrous ethanol (20 mL) and the TEOS solution was added dropwise to the $\text{Ti}_3\text{C}_2\text{T}_x$ dispersion with a dropwise acceleration of 1 drop/s. After the dropwise addition was completed, the temperature was raised to 35°C and the reaction was carried out for 4 h under magnetic stirring. When the reaction is finished, the above mixture was centrifuged several times and remove $\text{NH}_3\cdot\text{H}_2\text{O}$ and other by-products. Eventually, the sediment was dried under 60 °C to capture the hybrids $\text{Ti}_3\text{C}_2\text{T}_x@\text{SiO}_2$.

Preparation of PAA

The $\text{Ti}_3\text{C}_2\text{T}_x/\text{PI}$ composites were prepared in two steps: In the first step, ODA was pre-dried under vacuum at 80°C for 4 h. Similarly, PMDA was dried under vacuum at

100°C for 4 h. ODA (4 g) was added to DMAc (50 mL) and sonicated for 30 min until completely dissolved. Equimolar ratios of PMDA (4.36 g) were added to the ODA solution in three batches with high-speed stirring, and the addition was completed within 30 min. After the last addition, the speed was reduced to 80 rpm and the reaction was carried out under an ice-water bath for 3 h to obtain the polyamidoacetic acid (PAA) solution with 12% solid content.

Characterization

X-ray diffraction (XRD) patterns were recorded with a D8 Advance diffractometer, Cu was used as the target material with a scanning speed of 10°/min and a scanning interval of 5° to 70°. STP and transfer film were characterized with Thermo ESCALAB 250XI X-ray photoelectron spectroscopy (XPS) and LabRAM HR Evolution Raman Spectroscopy (the excitation wavelength was 633 nm). Morphology and microstructures were observed with a scanning electron microscope (SEM) (Gemini 300). Atomic force microscope (AFM) analysis of composite surface morphology using Bruker's Dimension XR model. FT-IR test was obtained from a NICOLET IS10 fourier transform infrared spectrometer (Nicolet, USA), and the scanning range was 4000~400 cm⁻¹, the number of scans was 32, and the resolution was 4.

Tribological tests

The friction coefficient and wear rate of the samples were tested by the friction and wear tester model MS-M9000 (Lanzhou, China). Friction experiments were conducted at room temperature using a 4 mm diameter bearing steel (GCr15) ball as the upper counterpart ball, a cured PI composite as surface film, and a steel (304) disc as the underlying counter facing plate. (The rotating speed was 300 r/min, and the rotating radius was 3 mm. The normal load was 5N, and the experimental duration was 30 min).

Table S1. The mass ratio of Ti₃C₂T_x-SiO₂/PTFE and samples name

| mass ratio | Sample |
|------------|---|
| 0:5 | PTFE |
| 1:4 | 1T-S/4P |
| 2:3 | 2T-S/3P |
| 3:2 | 3T-S/2P |
| 4:1 | 4T-S/1P |
| 5:0 | Ti ₃ C ₂ T _x -SiO ₂ |

The mass ratios of Ti₃C₂T_x-SiO₂/PTFE and the corresponding sample names are listed in **Table S1**. The tribological test results of the samples are shown in **Fig.S1**. The COF of the composites increased with the decrease of the percentage of PTFE (**Fig. S1a**), and the average wear rate was the lowest at the mass ratio of Ti₃C₂T_x-SiO₂ and PTFE of 3:2, which was $0.315 \times 10^{-5} \text{ mm}^3/(\text{N}\cdot\text{m})$ (**Fig. S1b**). Therefore, this ratio was comprehensively selected as the optimal ratio.

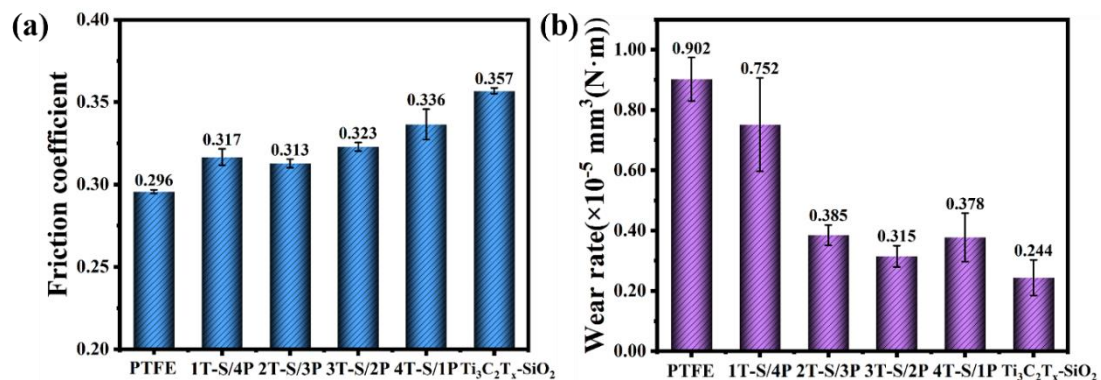


Fig. S1. Tribological properties of PI composites with different SiO₂-Ti₃C₂ and PTFE mass ratios. (a) COF; (b) wear rate.

Table S2. Roughness value of the STP/PI samples

| Sample | PI | STP1 | STP2 | STP3 | STP4 | STP5 | STP6 |
|-----------|------------|------------|------------|------------|------------|------------|------------|
| Ra | 0.42 | 2.81 | 3.71 | 4.77 | 4.81 | 4.97 | 5.93 |
| error bar | ± 0.03 | ± 0.06 | ± 0.11 | ± 0.02 | ± 0.08 | ± 0.10 | ± 0.47 |

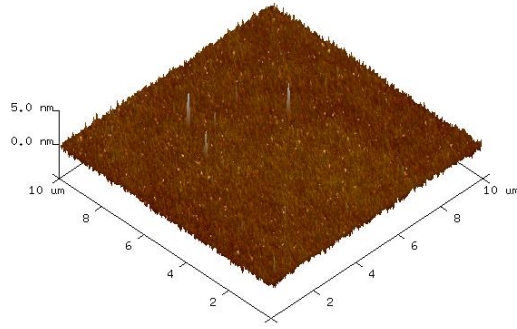


Fig. S2. AFM image of PI.

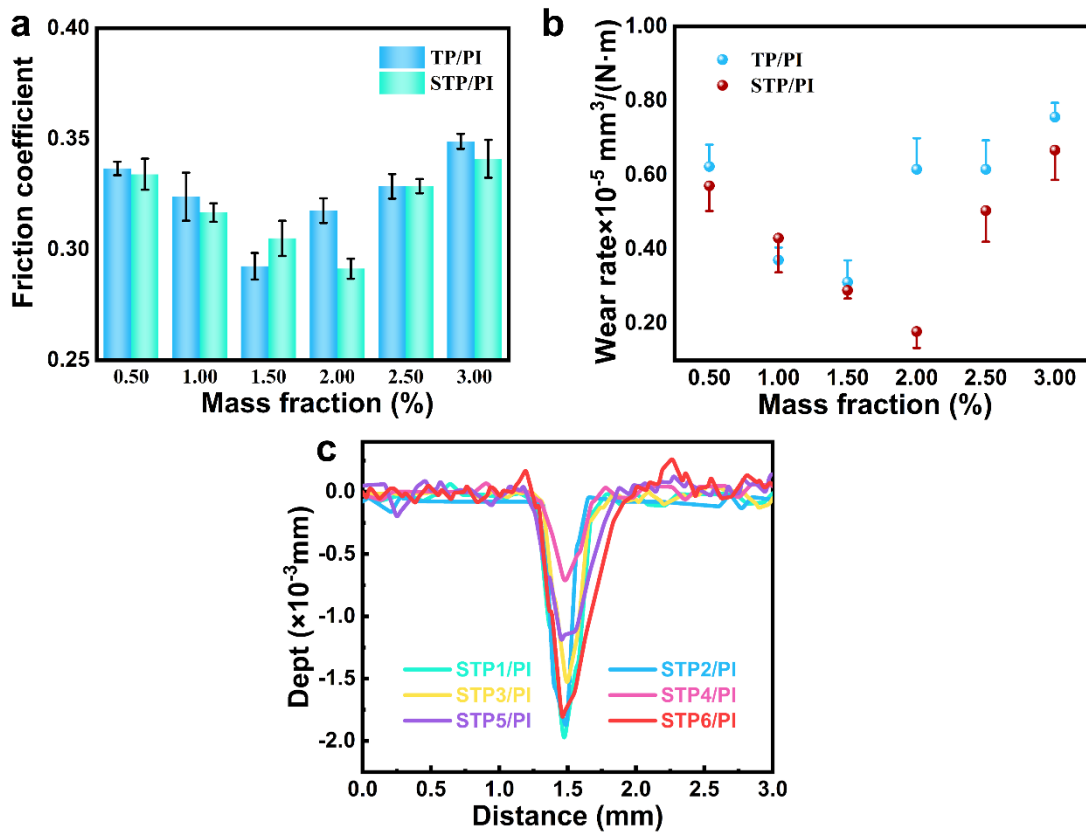


Fig.S3. Friction performance of TP/PI and STP/PI samples. (a) The COF comparison between TP/PI and STP/PI. (b) The wear rate comparison between TP/PI and STP/PI (c) Depth of the wear track of STP/PI.

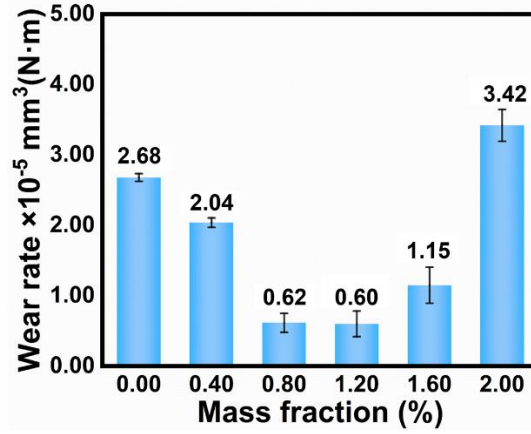


Fig. S4. Average wear rate of T/PI ($\text{Ti}_3\text{C}_2/\text{PI}$) with different Ti_3C_2 content

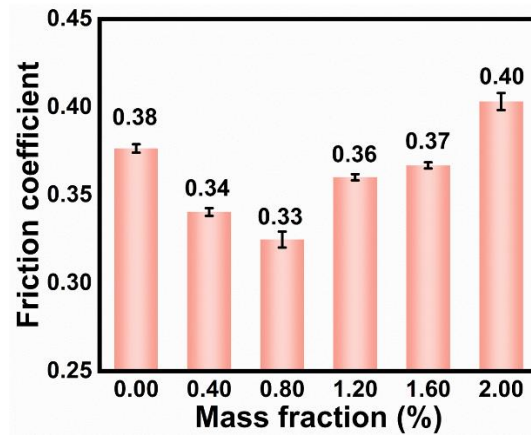


Fig. S5. Average coefficient of friction of ST/PI ($\text{Ti}_3\text{C}_2@\text{SiO}_2/\text{PI}$) with different $\text{Ti}_3\text{C}_2@\text{SiO}_2$ contents

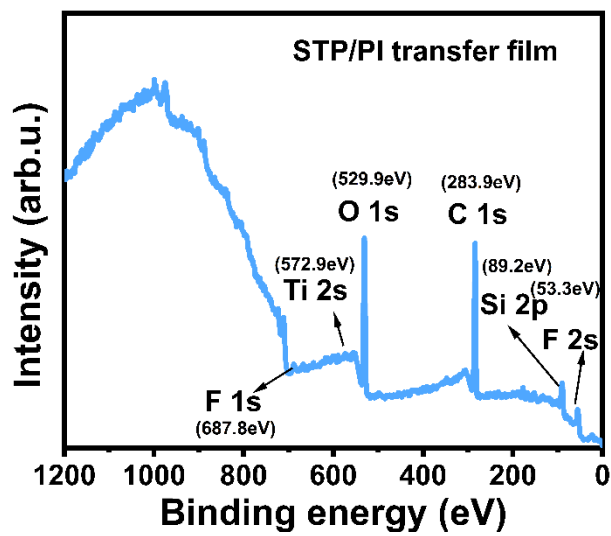


Fig. S6. XPS spectrum of transfer film on steel ball.

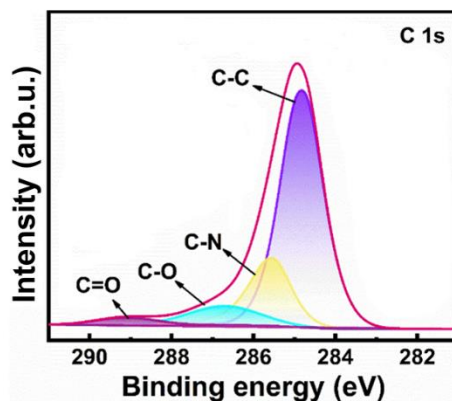


Fig. S7. XPS narrow spectrum of C1s from ST/PI transfer film

The Ti2p narrow spectrum can be divided into $Ti^{2+}2p_{3/2}$ (454.7 eV), $Ti^{2+}2p_{1/2}$ (461.9 eV), $Ti^{2+}2p_{3/2}$ (455.7 eV), $Ti^{2+}2p_{1/2}$ (461.4 eV), $Ti^{3+}2p_{3/2}$ (457.2 eV), $Ti^{3+}2p_{1/2}$ (464.9 eV), $Ti^{4+}2p_{3/2}$ (458.5 eV) and $Ti^{4+}2p_{1/2}$ (464.7 eV) due to energy level splitting. The peaks of Ti-O bonds are shown at 460.3 eV and 464.7 eV and the Ti-C bonds corresponds to 462.9 eV [1].

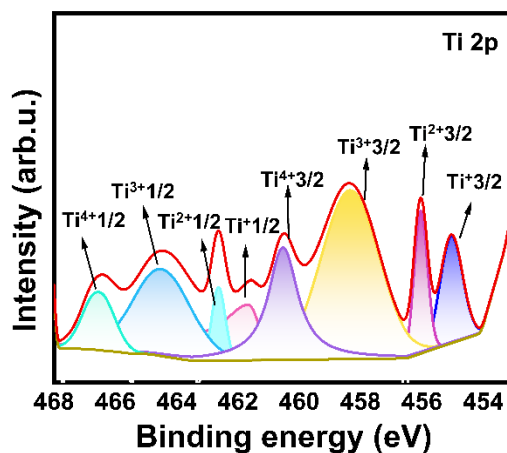


Fig. S8. XPS narrow spectrum (Ti2p) of the transfer film on steel ball

Table S3. Comparison of the tribological properties of this paper with other literatures

| Ref. | [2] | [3] | [4] | [5] | [6] | [7] | This work |
|-------------------------------|------|------|------|------|------|------|-----------|
| COF | 0.27 | 0.51 | 0.31 | 0.31 | 0.32 | 0.33 | 0.29 |
| Wear rate $\times 10^{-5}$ | 1.78 | 0.47 | 0.20 | 0.39 | 0.62 | 0.24 | 0.18 |

Compared with the work reported in recent years this study has some advantages in general, but the difference in data may be due to the difference in test loads. It is worthwhile to recognize that this work is a continuation of our group's previous work [6, 7] and is therefore comparable under the same testing conditions and sampling process. It can be seen that (**Table S3**) the tribological properties of STP as a solid lubricant are better than those of ST [7] and single MXene [6]. Therefore, this experimental data also proves that the addition of PTFE can effectively increase the interlayer movement of ST and MXene sheets.

References

- [1] X.L. He, J.X. Wu, S.H. Li, Y. Chen, L. Zhang, X.X. Sheng In-situ Growth of Aminated Silica on MXene Nanosheets: A novel 0D/2D Hybrid Structure for Multifunctional Waterborne Epoxy Composite Coatings. *Prog. Org. Coat.* 171 (2022) 107042.
- [2] K. Vishal, K. Rajkumar, P. Sabarinathan, Effect of Recovered Silicon Filler Inclusion on Mechanical and Tribological Properties of Polytetrafluoroethylene (PTFE) Composite, *Silicon*. 14 (2022) 4601–4610
- [3] C.P. Chai, Z.Q. Ma, X. Yin, H.S. Pang, Self-Lubricating and Self-Healing Polyurethane Nanocomposites Based on Aminated-Ti₃C₂Tx, <https://doi.org/10.1021/acsapm.3c02629>
- [4] Y.L. Zhao, X.W. Qi, Y Dong, J Ma, Q.L. Zhang, L.Z. Song, Y.L. Yang, Q.X. Yang, Mechanical, Thermal and Tribological Properties of Polyimide/nano-SiO₂ Composites Synthesized Using an In-situ Polymerization, *Tribol. Int.* 103 (2016) 599-608.
- [5] L.Y. Jin, X.R. Wang, Y.F. Huang, G.J. Chen, H.S. Pang, X. Yin, C.P. Chai Lubrication Mechanism of Polyimide/V₂CTx MXene Composites Based on Surface Chemistry, *Polym. Compos.* 44 (2023) 8075-8084.
- [6] G.J. Chen, S. Jiang, Y.F. Huang, H.S. Pang, X. Yin, C.P. Chai, Ultra-low Wear in Multifunctional Ti₃C₂Tx/PI Composite Films Induced by Tribo-chemistry Mechanism, *React. Funct. Polym.* 193 (2023) 105744.

[7] G.J. Chen, Z.Q. Ma, S. Jiang, X.R. Wang, Y.F. Huang, C.P. Chai, Highly lubricating and wear-resistant $\text{Ti}_3\text{C}_2\text{Tx}@/\text{SiO}_2/\text{PI}$ composites based on the action of transfer film at the friction surface, Polym. Compos. <https://doi.org/10.1002/pc.28200>.